Paper prepared for "FRONTIERS IN THE SCIENCE OF CLIMATE MODELING"
The Proceedings of a Symposium in Honor of Professor Robert D. Cess, Edited by J. T. Kiehl and V. Ramanathan
June 19, 2000 3:45 pm

Cloud Feedbacks

David A. Randall

Michael E. Schlesinger, Vener Galin, Valentin Meleshko,

Jean-Jacques Morcrette, Richard Wetherald

Abstract

Clouds affect climate through microphysical, radiative, and meso- and micro-scale dynamical processes. Cloud feedback occurs when one or more of these cloud-related processes changes systematically in response to some external forcing. External forcings of interest include the diurnal cycle, the seasonal cycle, volcanic eruptions, anthropogenic increases in greenhouse gases, and changes in the Earth's orbital parameters. The observational literature contains some evidence of cloud feedbacks on decadal time scales. Recent work shows that global atmospheric circulation models (AGCMs) are capable of simulating many observed fluctuations of cloudiness. When such models are coupled with ocean and land-surface models, and used in simulations of climate change, they produce simulations of cloud-climate feedback. These results can be analyzed, in terms of globally averaged quantities, using an approached developed to study feedbacks in linear systems. When such analyses are done for a collection of AGCMs, the results are found to differ widely among the models. Several specific cloud feedback hypotheses are discussed and critiqued. It is argued that the next generation of satellites will provide important new data relevant to cloud-feedback processes.

"An interpretation of climatological data suggests that cloud amount is not a significant climate feedback mechanism." -- R. D. Cess (1976).

1. Introduction

Although many of the best-known early climate models used prescribed clouds (e.g., Manabe and Bryan, 1969), the importance of potential changes in cloudiness for the problem of climate change has been recognized as a key factor since the 1970s (e.g., Arakawa, 1975; Charney et al. 1979). In particular, it is now widely appreciated that "cloud feedback" is a key source of uncertainty limiting the reliability of simulations of anthropogenic climate change (e.g., Houghton et al., 1990).

Nevertheless the whole concept of cloud feedback continues to be obscure, in part because the term "cloud feedback" is often used without being properly defined at all, and is rarely given a definition precise enough to show how it can be quantitatively measured. Further confusion arises from the fact that there are in fact many types of cloud feedbacks (e.g., Schneider, 1972; Schlesinger, 1985, 1988, 1989; Wielicki et al., 1995). In addition, it is widely perceived that existing atmospheric general circulation models (AGCMs) are incapable of making quantitatively realistic simulations of cloudiness.

The purposes of this Chapter are to give a definition of cloud feedback, to discuss some particular types of cloud feedback, and to assess the prospects for simulations of cloud feedback on anthropogenic climate change.

Before embarking on an exploration of the many problems in simulating cloud feedbacks, we would like to point out that there are reasons to believe that these problems can be and are being overcome. The AGCMs which are embedded in climate models are in principle identical to the AGCMs used for global numerical weather prediction (NWP). Miller et al. (1999) present comparisons of cloud forecasts performed with the NWP model of the European Centre for Medium Range Weather Forecasts (ECMWF) with cloud observations obtained through the Lidar-in-Space Technology Experiment (LITE; McCormick et al. 1993). The ECMWF model has high spatial resolution and incorporates many state-of-the-art physical parameterizations including the cloud parameterization of Tiedtke (1993). As shown in Fig. 1, the cloud forecasts are quite successful overall.

In addition, Klein and Jakob (1999) present statistical comparisons of a large number of ECMWF cloud forecasts with cloud observations in extratropical cyclones. Fig. 2 shows that again the cloud forecasts are very successful overall. It would be useful if the study of Klein and Jakob were extended to an analysis of the statistics of cloudiness in long "free runs" of the ECMWF model and/or other atmospheric GCMs. This would permit a comparison of the simulated and observed clouds associated with simulated and observed extratropical cyclones, respectively. Studies of this type, which relate to cloud feedbacks on synoptic time scales, will no doubt be carried out in the months and years ahead.

These studies demonstrate that GCMs can in fact predict realistic distributions of cloudiness in deterministic forecasts, for which the use of observed initial conditions ensures that the large-scale dynamical structures are realistic.

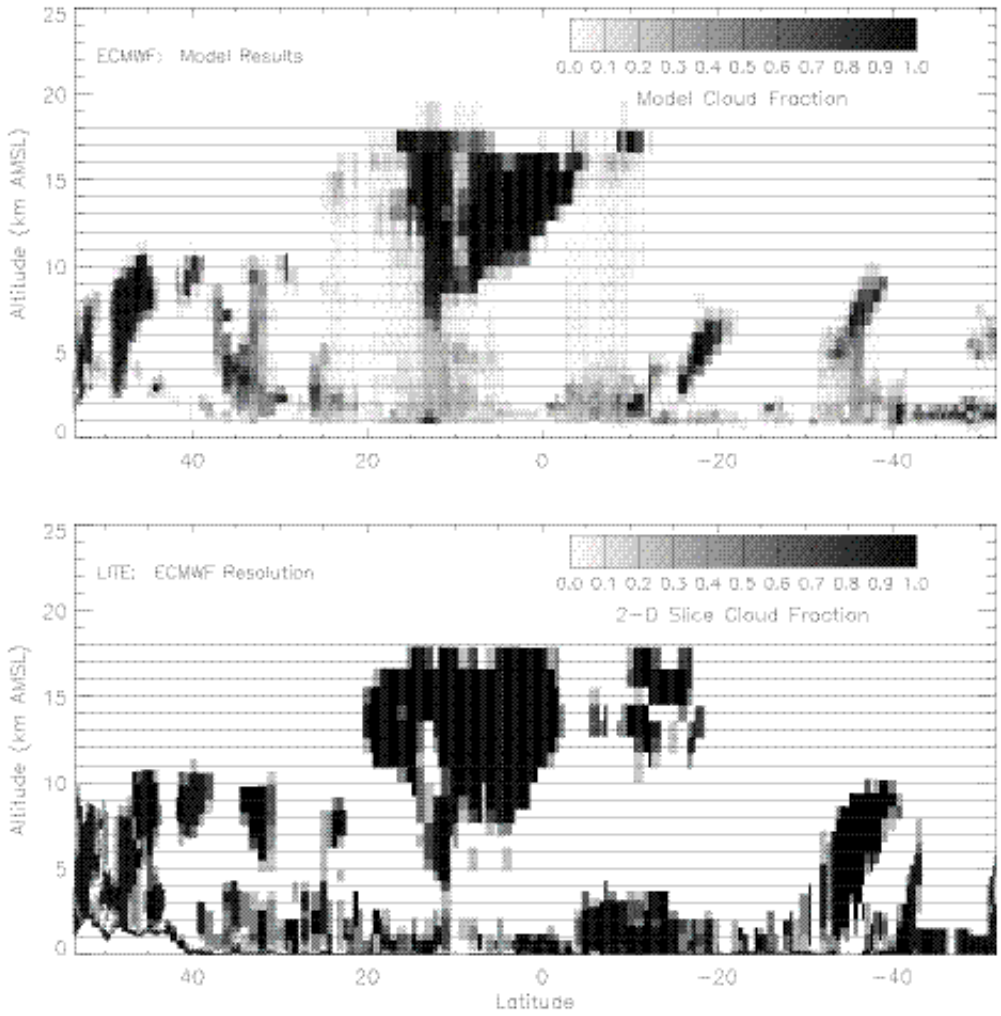

Fig. 1: **Cloud fraction comparison for LITE orbit 124 (September 16, 1994, 1425-1500 UTC, spanning the Wester Pacific warm pool). From Miller et al. (1999).**

While the results of Miller et al. (1999) and Klein and Jakob (1999) do not suffice to show that GCMs can realistically simulate changes in cloudiness that are associated with climate change, they are certainly promising and provide some grounds for optimism. In addition, they illustrate the enormous and as-yet-underexploited utility of NWP for the evaluation of parameterizations.

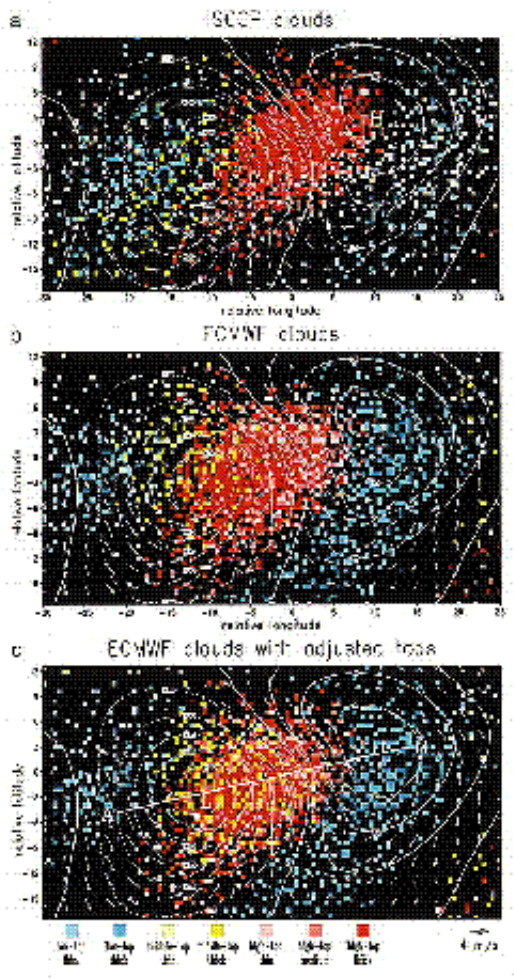

Fig. 2: **(a) Distributions of 1000-hPa horizontal wind (arrows, see scale at bottom right) and geopotential height (contours, interval 10 m) from ERA analyses, and various cloud types (color pixels) from ISCCP observations as shown in LC95. The ordinate (abscissa) of the coordinate system used here corresponds to latitudinal (longitudinal) displacements in degrees from the reference site. Inside each 2.5° by 2.5° grid box of this coordinate system, the presence and relative abundance of a certain cloud type is indicated by plotting a number of randomly scattered pixels with the color designated to the cloud species in questions (see legend at bottom). Each pixel represents a 1% increment in cloud fraction; negative values of cloud fraction are not plotted. In this and all following figures, the composite data for all fields represent deviations from background levels estimated by averaging the values for the 5-day period entered on the key dates. (b) As in panel a, but for cloud data and dynamical fields from the 24-h ERA forecasts. Clouds in this figure are classified by their physical cloud-top pressure. (c) As in Fig. 1b but using emissivity-adjusted cloud-top pressure. From Klein and Jakob (1999).**

2. The nature of cloud feedback

Clouds affect the Earth system in a variety of ways (Arakawa, 1975). They are produced by and are host to a wide variety of microphysical/hydrological processes, including most fundamentally latent heat release and precipitation. They strongly affect the flows of both longwave (LW) and shortwave (SW) radiation through the atmosphere. Finally, they are intimately associated with powerful microscale and mesoscale transport processes including deep penetrative convection (e.g., Arakawa and Schubert, 1974) and also the convective turbulence which fills stratiform clouds (e.g., Lilly, 1968), to the extent that a three-dimensional map of cloudiness is tantamount to a three-dimensional map of atmospheric turbulence (at least above the boundary-layer). The various cloud processes correspond to tendency terms in the equations describing the evolution of the atmosphere, the oceans, and the land surface. All three types of cloud processes -- microphysical/hydrological, radiative, and convective -- exert major influences on the climate system.

Because clouds are formed in and affect the atmospheric circulation, the effects of clouds on climate are fundamentally dynamical in character. Clouds couple many processes together, over a very wide range of space and time scales (Arakawa, 1975), giving rise to cloud-climate feedbacks, which are of intense interest in the context of anthropogenic climate change. Many types of cloud-climate feedbacks have been identified (e.g., Senior and Mitchell, 1993; Fowler and Randall, 1994; Yao and Del Genio, 1999; Senior et al., 1999), and probably there are some which have yet to be recognized. A survey is given by Wielicki et al. (1995). Since cloud influences involve microphysical and convective processes as well as radiative processes, cloud feedbacks are similarly diverse. For example, Schneider (1972) pointed out that cloud radiative feedbacks can occur through changes in cloud amount[1], cloud top-height, and cloud optical properties. Several specific types of cloud feedback are discussed later in this chapter. The various cloud feedbacks can interact with each other through their collective effects on the climate system as a whole.

[1.] Cess (1976) used an analysis of observations to conclude that cloud feedbacks due to changes in cloud amount are not significant, but further investigation has led him to change his mind about this (fervent personal communication on numerous occasions).

Any discussion of feedbacks in the climate system (or any other system) must carefully distinguish between internal and external processes. Internal processes are part-and-parcel of the system and so are affected by the state of the system and can interact with each other in potentially complex ways. External processes are unaffected by the state of the system. Only the interactive internal processes can "feed back" to influence the state of the system. The incident top-of-the-atmosphere solar radiation is perhaps the most obvious example of a potentially variable process external to the climate system. Cloud processes, on the other hand, are definitely internal to the climate system.

The effects of clouds are often discussed in terms of "cloud forcing," which refers to the effects of clouds on some climate process, most often the top-of-the-atmosphere radiation. As stressed above, cloud processes are internal to the climate system, and interact strongly with other climate processes. The term "forcing" has a strong connotation of externality. For this reason, we avoid using the term "cloud forcing." The effects of clouds on a process P will be denoted by $\boldsymbol{C}(P)$. For example, the effects of clouds on the outgoing longwave radiation will be represented by $\boldsymbol{C}(R_\infty)$, where R is the net upward longwave radiation (in general a function of height), and the subscript ∞ denotes the "top of the atmosphere". In addition, the symbol $\boldsymbol{C}$ (no parentheses and no argument) will be used to denote cloud influences in general.

The state of the climate system changes with time due to both internal processes and external forcing. For convenience, we refer to these as internal variability and external variability, respectively. Examples of internal variability (sometimes called "free" variability) include baroclinic wave development, tropical intraseasonal oscillations, and El Niño events. Familiar examples of time-dependent external forcing leading to external variability include the diurnal and seasonal cycles of solar forcing, and volcanic events, each of which can produce large-amplitude fluctuations of the climate system. We are particularly interested in the external variability due to the effects of the external forcings which arise from human activity and from the gradual changes in the Earth's orbital parameters.

Each of the various cloud processes mentioned earlier has the potential to change as the climate state evolves due to internal variability and/or externally forced variability. *The change in a cloud process associated with a fluctuation of the climate state represents a cloud-climate feedback*. Climate feedbacks, including cloud-climate feedbacks, thus help to determine the amplitude and character of both internal and external variability. For example, Hall and Manabe (1999) have shown that the internal (unforced) variability of a climate model becomes unrealistically weak when the water vapor feedback is artificially suppressed. Similarly, negative feedbacks act to reduce internal variability. This suggests that if clouds exert strong positive or negative feedbacks on climate, failure to represent these feedbacks in a model may result in unrealistically weak free fluctuations of the climate system, so that the internal variability of a simulated equilibrium climate state will be unrealistic. This illustrates the important point that cloud-climate feedbacks are at work even when a the climate system is in a statistical equilibrium. Cloud-climate feedbacks can thus influence the system even in the absence of climate change.

Cloud feedback as defined above is measurable, i.e., quantifiable from data, at least in principle; otherwise it would not be a proper subject for scientific study. Feedbacks are perhaps most readily measured through their influences on the internal and external variability of a system, i.e., by watching the system fluctuate. Cloud feedbacks on anthropogenic climate change can be observed by measuring the changes in cloud processes that occur over extended periods of time (decades or longer). Of course, we would like to measure the various cloud-climate feedbacks right now. One approach to doing so is to observe the changes in cloud processes which occur in the context of shorter-time-scale phenomena, such as El Niño events (e.g., Ramanathan and Collins, 1991), the seasonal cycle (e.g., Cess et al., 1997), various quasi-repeatable weather events (e.g., Klein and Jakob, 1999), and the diurnal cycle (e.g., Hendon and Woodberry, 1993). An understanding of how clouds feed back on these relatively "fast" processes can aid us in understanding how clouds feed back in the more ponderous processes of forced and unforced decadal and centennial variability.

Fig. 3 shows a possible example of an observed (Norris and Leovy, 1994) cloud feedback. The two panels of the figure show observed trends in sea-surface temperature (SST) and stratocumulus cloudiness, over a thirty-year period. Downward trends in sea surface temperature are correlated with upward trends in stratocumulus amount, and vice versa. There are at least two possible interpretations of these correlated trends in SST and stratocumulus cloud amount, which do not contradict each other. The first is that a cooling (warming) of the sea favors an increase (decrease) in stratus cloud amount; this is plausible in light of our understanding of the physics of marine stratus clouds. The second interpretation is that an increase (decrease) in stratus cloud amount favors a decrease (increase) in the sea surface temperature because the clouds reflect solar radiation which would otherwise be absorbed by the ocean.

In addition to measuring cloud-climate feedbacks, we would like to simulate them. Every climate-change simulation with a climate model produces a simulation of cloud-climate feedbacks, but we have to ask whether the simulated feedbacks will be found to agree with the observed ones, when suitable observations ultimately become available. Simulations also depict cloud feedbacks on shorter time scales. A demonstration that AGCMs can realistically simulate short-term cloud feedbacks is a positive (though not sufficient) indication that the same models can realistically simulate long-term cloud-climate feedbacks.

3. An example of simulated cloud feedbacks

Let R_∞ be the net upward LW radiation at the top of the atmosphere (TOA), S_∞ be the net downward SW radiation at the TOA, and $N \equiv S - R$ be the total radiation at the top of the atmosphere, positive downward. We also define $(R_\infty)_{\rm clr}$, $(S_\infty)_{\rm clr}$, and $(N_\infty)_{\rm clr}$ as the corresponding "clear-sky" fluxes, i.e., the fluxes which would occur if no clouds existed but the system was otherwise unchanged. Using the notation introduced earlier, cloud effects on the LW, SW, and net TOA radiation are then represented by

$$\boldsymbol{C}(R_\infty) \equiv R_\infty - (R_\infty)_{\rm clr}, \tag{1}$$

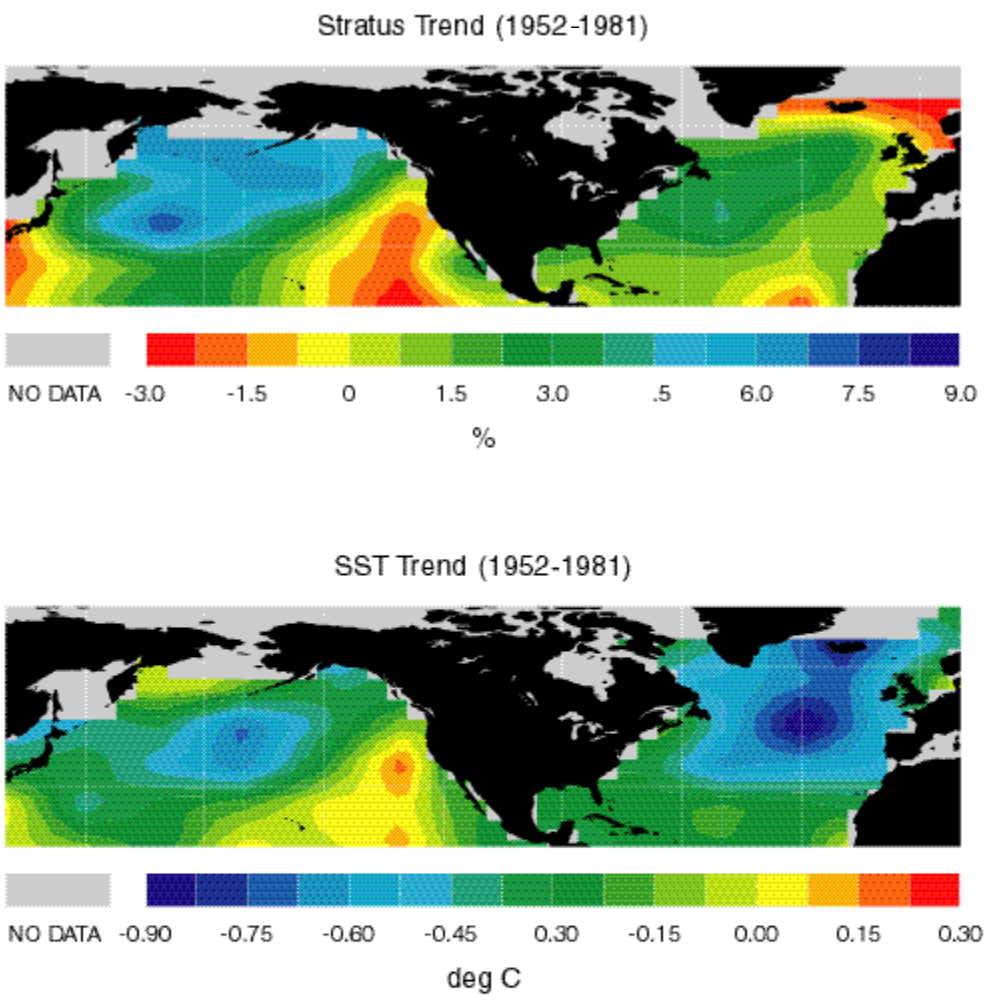

Fig. 3: **Observed trends of stratus cloud amount (top) and sea surface temperature (bottom), for the period 1952-1981. Adapted from Norris and Leovy (1994).**

$$\boldsymbol{C}(S_\infty) \equiv S_\infty - (S_\infty)_{\text{clr}}\,, \tag{2}$$

and

$$\boldsymbol{C}(N_\infty) \;=\; \boldsymbol{C}(S_\infty) - \boldsymbol{C}(R_\infty)\,, \tag{3}$$

respectively. With these definitions, we expect $\boldsymbol{C}(R_\infty) < 0$ and $\boldsymbol{C}(S_\infty) < 0$; it is observed that in

the global mean the $\boldsymbol{C}(S_\infty)$ dominates, so that the global mean of the $\boldsymbol{C}(N_\infty)$ is negative, i.e., clouds cool the Earth (e.g., Ramanathan et al. 1989).

As discussed above, we define a cloud feedback as the change in a cloud process that accompanies a climate change. With this definition, the cloud feedback is not simply a globally averaged quantity; it is a spatially and temporally varying field. As an example, Fig. 4 shows changes in zonally averaged low, middle, and high cloudiness as simulated by the Community Climate System Model (CCSM; Boville and Gent, 1998) when forced with a "21st-century" scenario (Dai et al., 2000) for increasing carbon dioxide (CO_2). A ten-year running mean has been applied to the model results. Low cloudiness tends to increase, particularly in the tropics, mid-level cloudiness decreases, particularly in middle latitudes, and high cloudiness increases, particularly in the Arctic. Note, however, that all of these simulated trends are rather weak. Fig. 5 shows the corresponding simulated trends in $\boldsymbol{C}(S_\infty)$, $-\boldsymbol{C}(R_\infty)$, and $\boldsymbol{C}(N_\infty)$. Again, the trends are weak. This model produces only weak cloud-climate feedbacks in terms of the radiation at the top of the atmosphere. In the future it will become possible to compare such model results with observations.

4. Linear systems analysis of climate feedbacks

Schlesinger (1985, 1988, 1989) defined and analyzed climate feedbacks, including the cloud-climate feedback, using linear systems analysis (e.g., Bode, 1975), whereby feedback is quantified in terms of partial derivatives which represent the rates of response of internal variables to changes in external forcing. A summary of this approach is given by Curry and Webster (1999). The concepts can be understood with reference to a simple model of the climate system, in which the Earth is considered as a point-like body in space, receiving an insolation $S\downarrow_\infty$, with a planetary albedo α, a bulk emissivity ε, and a global-mean surface temperature T_S, such that the globally averaged outgoing longwave radiation per unit area, R_∞, is given by

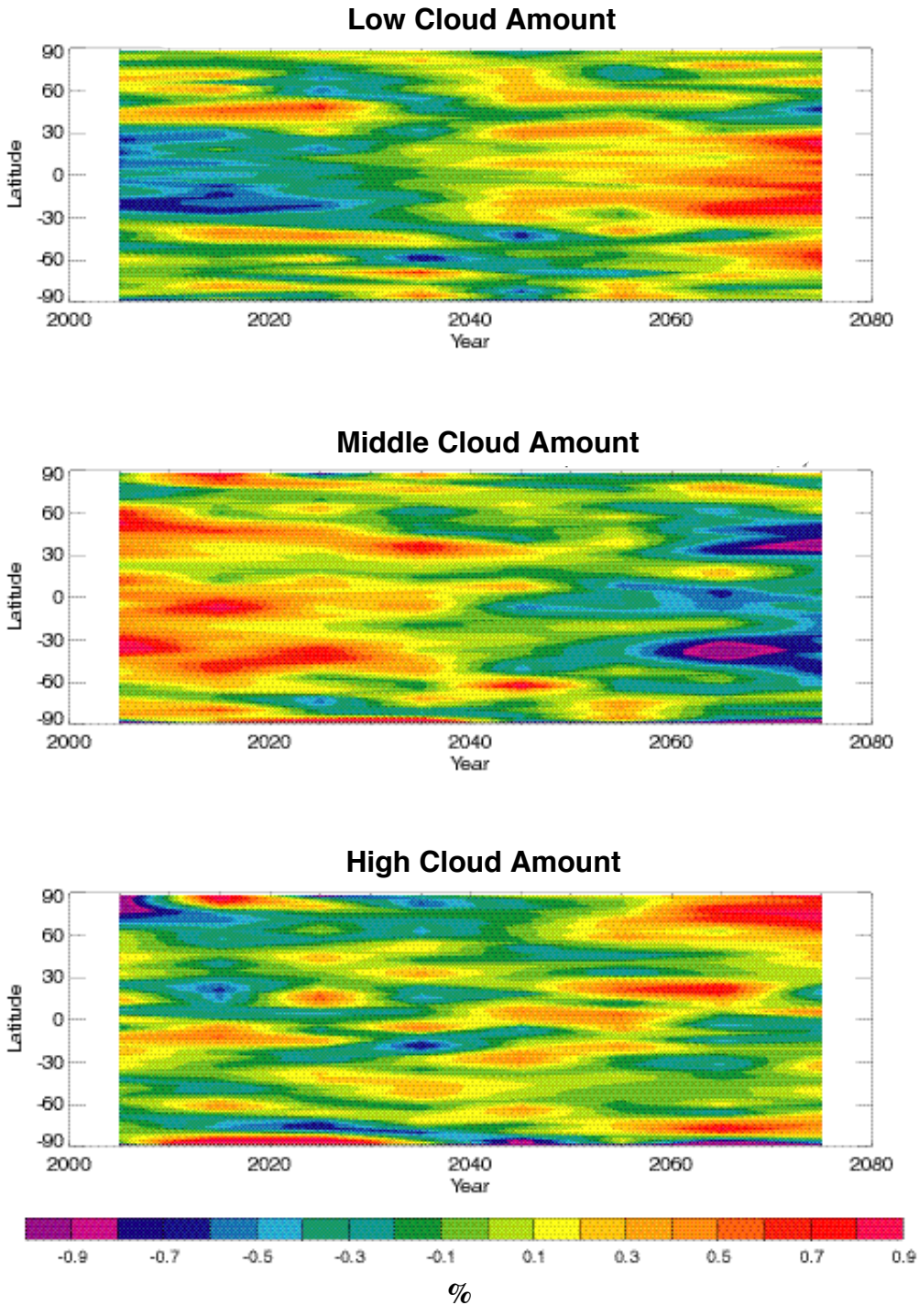

Fig. 4: **Zonally averaged changes in low, middle, and high cloud amount, as simulated by the CCSM. The plots show the departures from the time mean at each latitude.**

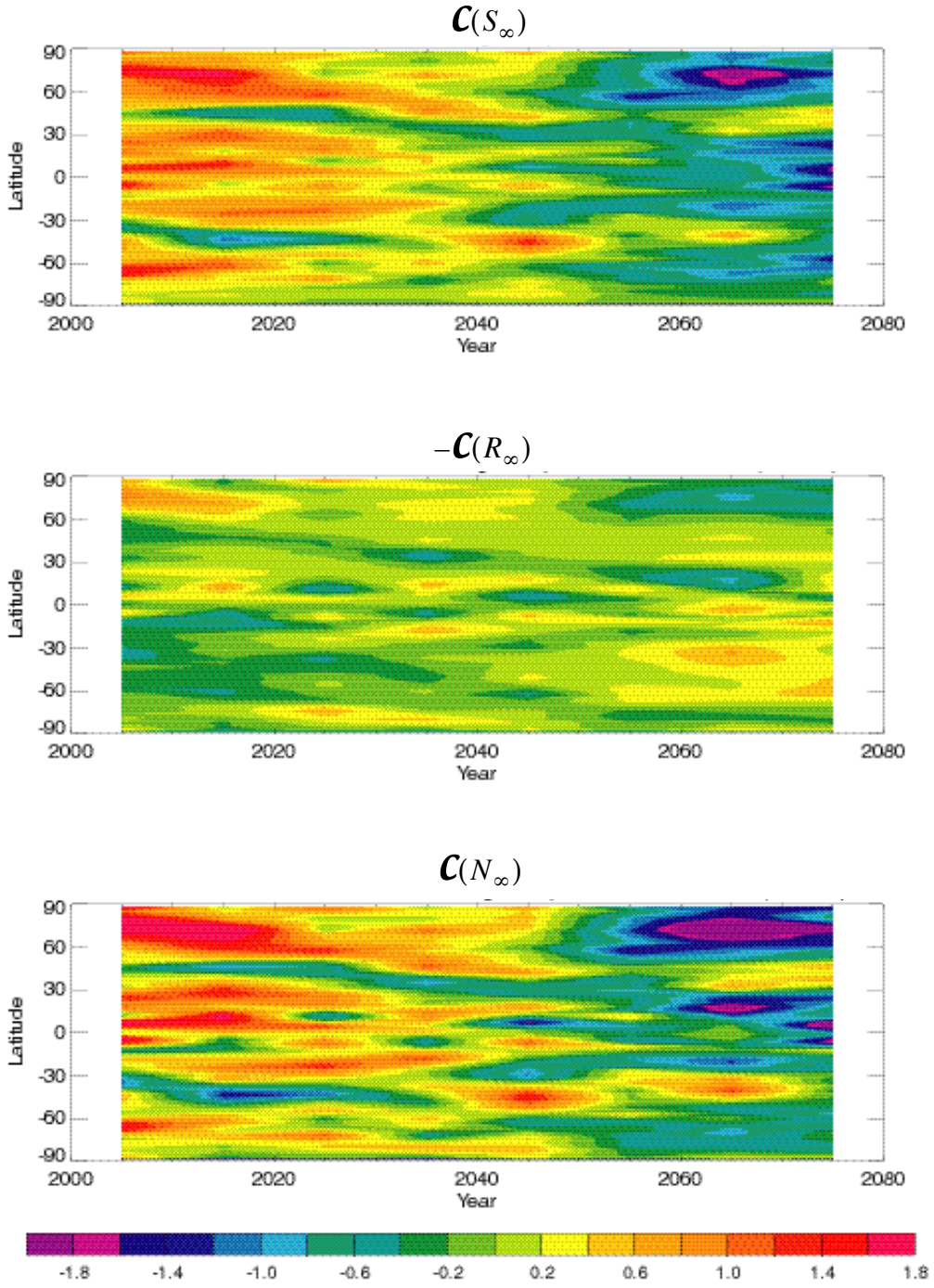

Fig. 5: **As in Fig. 4, but for the trends of, $C(S_\infty)$, $-C(R_\infty)$, and $C(N_\infty)$. Note that $-C(R_\infty)$ is what is sometimes called the "longwave cloud forcing".**

$$R_\infty = \varepsilon\sigma T_S^4 . \tag{4}$$

Here σ is the Stefan-Boltzmann constant. For the Earth, $S\downarrow_\infty = 1370$ W m^{-2}, $\alpha = 0.3$, $T_S = 288$ K, $\varepsilon = 0.6$, and $R_\infty = 240$ W m^{-2}. The radiation budget in equilibrium is expressed by $\pi a^2 S\downarrow_\infty (1-\alpha) = 4\pi a^2 \varepsilon\sigma T_S^4$, where a is the radius of the Earth. After simplifying, we find that

$$4\varepsilon\sigma T_S^4 = S\downarrow_\infty (1-\alpha) = S_\infty . \tag{5}$$

In (5), T_S is clearly an internal variable, and $S\downarrow_\infty$ is clearly an external variable.

We linearize about an equilibrium "base" state in which $S\downarrow_\infty = S\downarrow_0$, $\alpha = \alpha_0$, $\varepsilon = \varepsilon_0$, and $T_S = T_0$, so that the base state satisfies

$$4\varepsilon_0\sigma T_0^4 = S\downarrow_0 (1-\alpha_0) . \tag{6}$$

A linearized version of (5) is

$$16\varepsilon_0\sigma T_0^3 \Delta T_S + 4\Delta\varepsilon\sigma T_0^4 = \Delta S\downarrow (1-\alpha_0) - S\downarrow_0 \Delta\alpha \quad . \tag{7}$$

Here $\Delta S\downarrow$ is the perturbation to $S\downarrow_\infty$, and ΔT_S, $\Delta\varepsilon$, and $\Delta\alpha$ are defined similarly. The left-hand side of (7) represents the perturbation of R_∞, and the right-hand side represents the perturbation of $S\downarrow_\infty$. Note that the implied perturbation of N_∞ is zero, because we assume that both the base

state and the perturbed state are in equilibrium.

The bulk emissivity can have both an externally modulated component (e.g., due to anthropogenic changes in CO_2) and an internally varying component (e.g., due to changing amounts of cloudiness and/or water vapor), so that we can write

$$\Delta\varepsilon = (\Delta\varepsilon)_{\text{ext}} + (\Delta\varepsilon)_{\text{int}} . \tag{8}$$

Similarly, the planetary albedo can have both an externally modulated component (e.g., due to volcanic events) and an internally varying component (e.g., due to changes in cloudiness and/or snow and ice cover):

$$\Delta\alpha = (\Delta\alpha)_{\text{ext}} + (\Delta\alpha)_{\text{int}} . \tag{9}$$

An external perturbation or "forcing" of the system can arise from one or more of several possible causes: changes in $S\downarrow_{\infty}$ from its nominal value $S\downarrow_0$, and/or non-zero values of $(\Delta\varepsilon)_{\text{ext}}$, and/or non-zero values of $(\Delta\alpha)_{\text{ext}}$. The response of the system can be measured in terms of the *equilibrium* changes in the various internal variables, which are T_S, ε_{int}, and α_{int}.

Now introduce feedbacks. Let

$$\begin{aligned} (\Delta\alpha)_{\text{int}} &= (\Delta\alpha)_{\text{ice, clr}} - \frac{\Delta[\boldsymbol{C}(S_{\infty})]}{S\downarrow_0} , \\ &= -I\Delta T_S - A\Delta T_S \end{aligned} \tag{10}$$

and

$$\begin{aligned} \Delta\varepsilon &= (\Delta\varepsilon)_{\mathrm{CO_2,\,clr}} + (\Delta\varepsilon)_{\mathrm{int}} \\ &= (\Delta\varepsilon)_{\mathrm{CO_2,\,clr}} + (\Delta\varepsilon)_{\mathrm{vap,\,clr}} + \frac{\Delta[\boldsymbol{C}(R_\infty)]}{\sigma T_0^{\,4}} \\ &= (\Delta\varepsilon)_{\mathrm{CO_2,\,clr}} - V\Delta T_S - E\Delta T_S \quad , \end{aligned} \tag{11}$$

where $(\Delta\alpha)_{\mathrm{ice,\,clr}} = -I\Delta T_S$ represents the change in the *clear-sky* albedo due to melting ice and snow, $(\Delta\varepsilon)_{\mathrm{CO_2,\,clr}}$ represents the externally forced change in the *clear-sky* bulk emittance due to changes in the atmospheric CO_2 concentration, and $(\Delta\varepsilon)_{\mathrm{vap,\,clr}} = -V\Delta T_S$ represents the change in the *clear-sky* bulk emittance due to the changing water vapor content of the atmosphere. The notation $\Delta[\boldsymbol{C}(S_\infty)]$ means the perturbation to $\boldsymbol{C}(S_\infty)$, and $\Delta[\boldsymbol{C}(R_\infty)]$ is defined similarly. The quantities A, I, E, and V are essentially partial derivatives. For example,

$$E\Delta T_S = -\frac{\Delta[\boldsymbol{C}(R_\infty)]}{\sigma T_0^{\,4}}, \tag{12}$$

which implies that

$$E = \frac{-1}{\sigma T_0^{\,4}} \frac{\Delta[\boldsymbol{C}(R_\infty)]}{\Delta T_S}, \tag{13}$$

i.e., E is a normalized partial derivative of $\boldsymbol{C}(R_\infty)$ with respect to T_S. Similarly,

$$A = \frac{1}{S\downarrow_0} \frac{\Delta\boldsymbol{C}(S_\infty)}{\Delta T_S} \tag{14}$$

is a normalized partial derivative of $\Delta C(S_\infty)$ with respect to T_S.

In (10) and (11) we have assumed that $(\Delta\alpha)_{\text{int}}$ and $(\Delta\varepsilon)_{\text{int}}$ can be written as functions of T_S only. Given the overwhelming complexity of the climate system, this appears to be a rather drastic assumption. It can be rationalized to some extent, however, by thinking of T_S as an "index" of the climate equilibrium state; the linearization used above will be useful to the extent that $(\Delta\alpha)_{\text{int}}$ and $(\Delta\varepsilon)_{\text{int}}$ have one-to-one (i.e., single-valued) relationships with T_S in the neighborhood of the base state about which the linearization is performed. The existence of such one-to-one relationships is plausible, if by no means assured.

It should also be noted that our analysis is linear. Equation (7) was derived through linearization of the Planck function. Moreover, we are representing the feedbacks as first-order derivatives of T_S in the vicinity of the base state; we neglect higher-than-first-order derivatives, which is an acceptable approximation if ΔT_S is sufficiently small. These linearized feedbacks are conceptually compatible with the linearization already used to obtain (7). Note, however, that feedbacks in the real climate system, when subjected to real perturbations of interest, may or may not behave linearly.

With the use of (10) and (11), Eq. (7) can be written as

$$\begin{aligned} 16\varepsilon_0\sigma T_0^3\Delta T_S + 4\sigma T_0^4[(\Delta\varepsilon)_{\text{CO}_2,\,\text{clr}} - (E+V)\Delta T_S] \\ = \Delta S\downarrow(1-\alpha_0) + S\downarrow_0[(A+I)\Delta T_S] \quad , \end{aligned} \tag{15}$$

which can be solved for ΔT_S, yielding

$$\Delta T_S = \frac{G_0\left[-\sigma T_0^4(\Delta\varepsilon)_{CO_2,\,clr} + \frac{\Delta S\downarrow(1-\alpha_0)}{4}\right]}{1 - G_0 F}, \tag{16}$$

where we define

$$G_0 \equiv \frac{T_0}{4\varepsilon_0\sigma T_0^4} = \frac{T_0}{(1-\alpha_0)S\downarrow_0} = 0.3 \text{ K (W m}^{-2})^{-1} \tag{17}$$

and

$$F = \sigma T_0^4(E+V) + \frac{S\downarrow_0}{4}(A+I). \tag{18}$$

External forcing enters through the numerator of (16); in fact, $-4\sigma T_0^4(\Delta\varepsilon)_{CO_2,\,clr} - \Delta S\downarrow(1-\alpha_0)$ is the change in N_∞ which would occur *instantaneously* if the imposed forcing were suddenly "switched on." Of course, after equilibration the change in N_∞ must be zero. Feedbacks enter through the denominator of (16), via the parameter F, which is given, according to (18), in terms of A, I, E, and V. We can thus identify A, I, E, and V as "feedback parameters."

Equations (13) and (14) show how the feedback parameters E and A can be computed in terms of partial derivatives; similar formulae can be given for I and V. Also note that the various feedbacks simply add in (18). Positive (negative) values of either $A+I$, or $E+V$ will give positive (negative) feedbacks. The cloud feedback parameters are A and E.

We can imagine a case in which the feedbacks make the denominator of (16) zero, implying an infinite response to a finite forcing. One interpretation would be that the climate system will be unable to achieve equilibrium with the perturbed forcing. A more modest interpretation would be that the linearizations used in the derivation of the model cause the analysis to break down in such a case.

For a CO_2 perturbation in the absence of feedbacks, (16) reduces to

$$\Delta T_S = -G_0[(\Delta\varepsilon)_{CO_2,\,clr}\sigma T_0^4] = \frac{-T_0}{4}\left[\frac{(\Delta\varepsilon)_{CO_2,\,clr}}{\varepsilon_0}\right]. \tag{19}$$

If we instantaneously double CO_2, the effect is to reduce ε in such a way that R_∞ instantaneously decreases by about 4 W m^{-2}, thus disrupting the equilibrium. Therefore (19) gives

$$\Delta T_S = 0.3 \text{ K/(W m}^{-2})(4 \text{ W m}^{-2}) = 1.2 \text{ K}. \tag{20}$$

Feedbacks can either increase or decrease this response.

We now give a graphical interpretation of the preceding discussion. Consider the two "block diagrams" shown in Fig. 6, which can be considered as an illustration of the linearized model discussed above. The diagram illustrates the logical structure of a system which is subjected to a forcing and produces a response. The system's response to external forcing is determined by the "transfer function," G_0, defined by (16), and also called the "zero-feedback gain." Feedbacks are represented by F.

The upper diagram in Fig. 6 illustrates the base state of the system, in which external forcings given by $S\downarrow_0$ and ε_0 give rise to a response T_0. (We write the infrared part of the

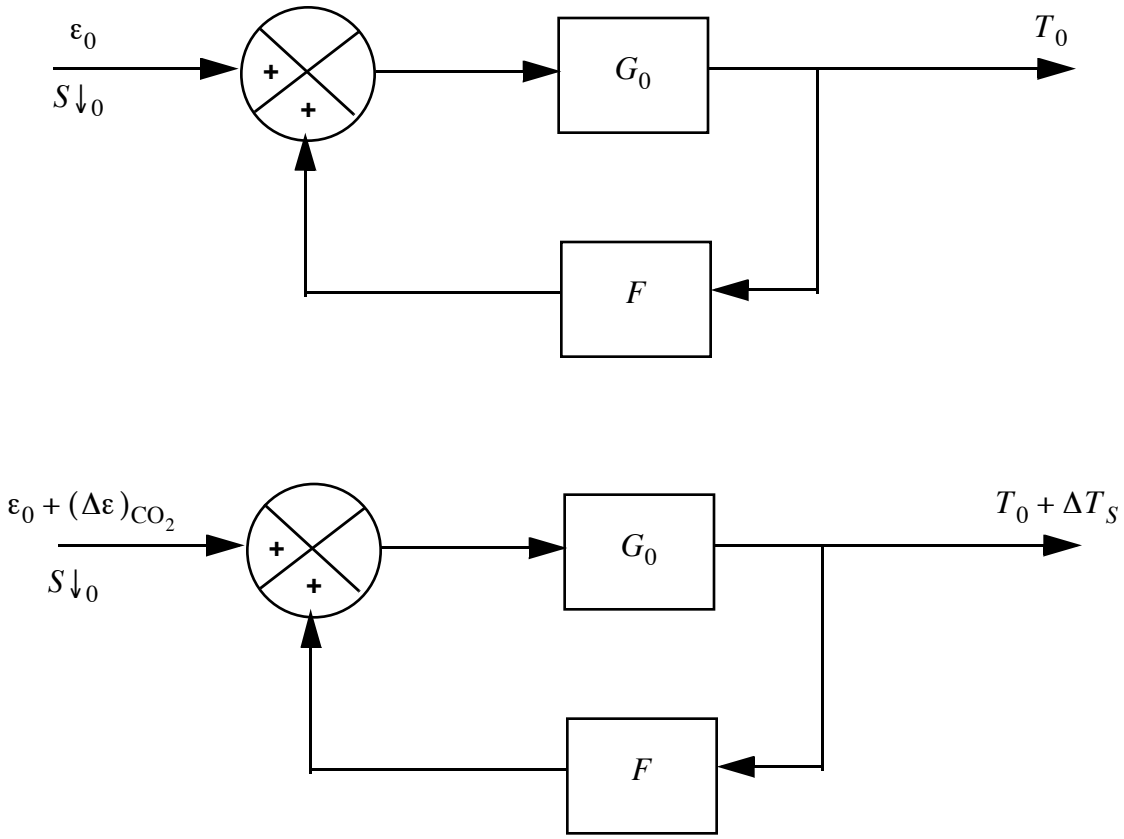

Fig. 6: **"Block diagrams" illustrating the approach of linear systems analysis to the analysis of climate feedbacks. In the upper diagram, the external forcing consists of the incident solar radiation, $S\downarrow_0$, and a particular atmospheric composition which gives rise to the bulk emissivity ε_0. The response of the system to the forcing is measured in terms of the surface temperature T_S, which is (necessarily) an internal parameter. The parameter G_0 is a "transfer function" which relates the forcing to the response; it is the "gain", which can be defined as the response divided by the forcing, in the absence of feedback. The lower diagram shows a perturbed state of the system. In the lower diagram, $(\Delta\varepsilon)_{CO_2,\,clr}$ and ΔT_S represent perturbations to the forcing and the response, respectively. In this example the solar forcing is assumed to be unperturbed. The feedback of the system is represented by F. See text for details. Adapted from Schlesinger (1985, 1988, 1989).**

forcing as ε_0 rather than as $\varepsilon_0 \sigma T_0^4$ because the latter form would express the forcing partly in terms of an internal parameter, namely T_0.) The base state satisfies

$$T_0 = G_0 S\downarrow_0 (1 - \alpha_0) . \tag{21}$$

Note that the feedback parameter, F, does not appear in this equation. The perturbation (relative to the base state) forcing in the lower panel of Fig. 6 is given by $(\Delta\varepsilon)_{CO_2, clr}$; for simplicity, we have assumed that $\Delta S\downarrow = 0$. In the absence of feedback the response of the climate system to the perturbation of the forcing is given by (19). When feedback is active (i.e., for $F \neq 0$), ΔT_S is altered to

$$\Delta T_S = G_0[-\sigma T_0^4 (\Delta\varepsilon)_{CO_2, clr} + F\Delta T_S] , \tag{22}$$

so that

$$\Delta T_S = \frac{-G_0 \sigma T_0^4 (\Delta\varepsilon)_{CO_2, clr}}{1 - G_0 F} . \tag{23}$$

Compare with (16). The feedback parameter does appear in (23), but it did not appear in (21). Note that the physical processes which give rise to feedback are operating in both the base state and the perturbed state.

The coefficients A and E were introduced by way of linearization; they essentially represent partial derivatives of the albedo and emissivity, respectively, with respect to the surface

temperature, which is used here as a sole indicator of the climate state. It is feasible to evaluate these partial derivatives through the use of models; examples are given by Schlesinger (1985, 1988, 1989) and Curry and Webster (1999). It is also possible to evaluate the partial derivatives through the use of data.

The linear systems analysis does not in itself explicitly represent the physical processes responsible for the various feedbacks. The complex physical processes associated with cloud and water-vapor feedbacks are (purportedly) included in detailed climate models, and attempts have been made to incorporate them into simple climate models (e.g. Kelly et al., 1999).

Note, however, that the preceding discussion of cloud feedback in terms of linear systems analysis is formulated entirely in terms of globally averaged quantities. In practice we are interested in analyzing the external forcing, the response, and the feedbacks *as spatially distributed fields*. In fact, an understanding of spatial variations of $\boldsymbol{C}(R_\infty)$, $\boldsymbol{C}(S_\infty)$, and $\boldsymbol{C}(N_\infty)$, and other measures of cloud feedback is necessary because of the Earth's wide variety of cloud regimes and the very different circulation regimes in which they occur. It must be expected that the surface temperature and various feedbacks, including cloud feedbacks, would vary in spatially and/or seasonally correlated ways. In addition, we must understand the physical processes at work in producing these spatially distributed fields. Linear systems analysis does not address these processes.

As an example, consider the potential contribution to cloud-climate feedback of a possible change in $\boldsymbol{C}(S_\infty)$ over the eastern North Pacific Ocean, associated with changes in the amount of marine stratocumulus cloudiness there. Among the parameters which are believed to affect marine stratocumulus cloud amount are the sea surface temperature, the large-scale vertical motion, the temperature and moisture jumps across the top of the marine layer, the tendencies of marine-layer temperature and moisture due to horizontal advection, and the wind speed and direction including the shear across the top of the marine layer. These quantities are, in turn,

affected by various processes in remote locations on the Earth; for example, the large-scale vertical motion over the eastern North Pacific Ocean is affected by the strength of the North American Monsoon (e.g., Rodwell and Hoskins, 2000).

Despite this complexity, the geographical structure of cloud feedback can be observed, simulated, and otherwise analyzed. For example, the spatial distributions of $\boldsymbol{C}(R_\infty)$, $\boldsymbol{C}(S_\infty)$, and $\boldsymbol{C}(N_\infty)$, and their changes over time, can be studied through both observational and modeling approaches. An example has already been provided in Fig. 5.

5. Can we accurately simulate cloud-climate feedbacks?

In a widely cited analysis, Cess et al. (1989, 1990; hereafter C89) presented the results of idealized numerical experiments designed to investigate the role of cloud feedback in climate change. The experiments were performed with more than a dozen AGCMs, and in fact C89 was the first and one of the most successful "intercomparison" activities undertaken by the AGCM community.

Among the most fundamental aspects of climate change is the complex seasonally varying spatial pattern of changes in the SST distribution. A climate forcing, such as the TOA radiation changes associated with increased CO_2, leads, through a complex process with a lag time of decades, to changes in the SST. In order to predict how the SST changes in response to the imposed radiative forcing, climate models must include ocean sub-models. C89 cleverly elected to "solve the problem backwards" by prescribing the SST change in a simplified manner, and computing the implied TOA radiative forcing. This elegant strategy eliminates the need for ocean sub-models and long integrations. For simplicity, C89 prescribed globally uniform changes in the SST, and made runs with SSTs increased by 2 K, decreased by 2 K, and also fixed at their observed (July) values. For further discussion of the experiment design, see C89.

C89 defined a "climate-sensitivity parameter," λ, as the ratio of ΔT_S to ΔQ, which is defined as the imposed *instantaneous* change in N_∞ which would occur if the forcing were suddenly switched on; once again, it is important to keep in mind that in equilibrium $N_\infty = 0$ and, therefore, $\Delta N_\infty = 0$. In the parlance of linear systems analysis,

$$\lambda = \frac{\Delta T_S}{\Delta Q} = \frac{G_0}{1 - f}, \tag{24}$$

where $f = G_0 F$. Consistent with the discussion given the preceding sub-section, C89 defined the cloud feedback in terms of the change in the globally averaged $\boldsymbol{C}(N_\infty)$, i.e. $\Delta[\boldsymbol{C}(N_\infty)]$, in response to the imposed SST changes.

Because of the idealized nature of C89's experiment, the results cannot be used to draw any conclusions about real climate change scenarios. The idealizations drastically simplify the interpretation of the results, however, and do in fact permit interesting and important conclusions to be drawn. The key findings of C89 can be summarized as follows:

- The climate-sensitivity parameter varied by roughly a factor of three among the models.

- Inter-model differences in the cloud feedback accounted for almost all of the inter-model differences in the climate-sensitivity parameter. This is illustrated in Fig. 7.

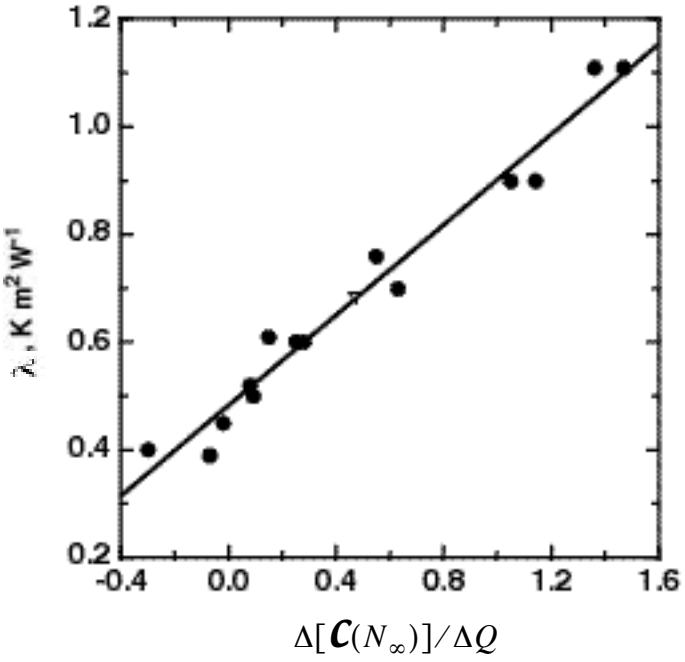

Fig. 7: The climate-sensitivity parameter λ plotted against the cloud-feedback parameter $\Delta[\boldsymbol{C}(N_\infty)]/\Delta Q$ produced in 14 GCM simulations. From Cess et al. (1989).

- The "clear-sky" climate-sensitivity parameter, defined by analogy with λ but using the clear-sky TOA radiation in place of the all-sky TOA radiation, agreed very well among the models.

Cess et al. (1996) showed that updated versions of the AGCMs exhibit smaller inter-model differences; Cess et al. (1996) note, however, that this does not necessarily indicate that we have arrived at a better understanding of the cloud-climate feedback problem. In a follow-up study, Cess et al. (1997) presented results from a further intercomparison based on simulated (and observed) changes in the $\boldsymbol{C}(N_\infty)$ in response to a realistic *seasonal* change, rather than an idealized climate change. They concluded that none of the models realistically reproduced the observed seasonally varying $\boldsymbol{C}(N_\infty)$, although some did better than others.

On the basis of the results of C89 and Cess et al. (1996), the question posed by the title of this section, i.e., "Can we accurately simulate cloud-climate feedbacks," must be answered: "In view of the discrepancies among the model results, at least some of the current models cannot accurately simulate cloud-climate feedbacks, and it remains to be seen whether any of them can."

A limitation of the studies discussed above is that none of them focused on specific cloud-climate-feedback mechanisms. We now consider several such mechanisms.

6. A global radiative-convective feedback

The observed globally averaged energy budgets of the Earth's surface and the atmosphere are discussed, for example, by Peixoto and Oort (1992). For the Earth's surface, the globally averaged net radiative heating approximately balances the globally averaged evaporative cooling.[2] For the atmosphere, the globally averaged net radiative cooling approximately balances the globally averaged latent-heat release.[3] In short, the hydrologic cycle plays a dominant role in the energy budgets of both the Earth's surface and the atmosphere.

Radiatively active clouds are themselves products of the hydrologic cycle. The clouds strongly modulate both the net surface radiative heating and the net atmospheric radiative cooling. Clouds reduce the solar radiation absorbed by the Earth's surface, but increase the net infrared radiation impinging on the surface. Clouds reduce the solar radiation absorbed by water vapor in the lower troposphere, and they also warm the atmosphere by reducing the infrared emission to space by water vapor and CO_2.

We now explore these ideas more quantitatively, but still in a simplified framework. As discussed above, the globally averaged *atmospheric* energy balance is approximately expressed by

---

2. The surface sensible heat flux plays a relatively small role in the global-mean surface-energy budget, although it can be very important locally.

3. The surface sensible heat flux plays a relatively small role in the global mean atmospheric energy budget.

$$SW_{atm} - LW_{atm} + LP \cong 0 \,. \tag{25}$$

Here $SW_{atm} \equiv S_\infty - S_S$ and $LW_{atm} \equiv R_\infty - R_S$ are the globally averaged net SW heating and LW cooling of the atmosphere, respectively, and LP is the globally averaged net latent heating of the atmosphere. Each of these quantities is an energy flux. We can make cloud effects explicit by writing

$$SW_{atm} - LW_{atm} \cong SW_{atmclr} - LW_{atmclr} - \boldsymbol{C}(R_\infty) + \boldsymbol{C}(S_\infty - S_S) \,. \tag{26}$$

Here SW_{atmclr} and LW_{atmclr} are the clear-sky net SW heating and LW cooling of the global atmosphere, respectively. We assume here, for simplicity, that $\boldsymbol{C}(S_\infty - S_S)$ is negligible and that $\boldsymbol{C}(R_\infty)$ modulates the longwave cooling of the atmosphere. For example, an increase in cirrus cloudiness will cause $\boldsymbol{C}(R_\infty)$ to become more negative, and this will tend to reduce the net radiative cooling of the atmosphere.

Both precipitation and $\boldsymbol{C}(R_\infty)$ are associated with deep convection, so it is useful to define

$$\beta \equiv \frac{-\boldsymbol{C}(R_\infty)}{LP} \cong \frac{30 \text{ W m}^{-2}}{90 \text{ W m}^{-2}} = \frac{1}{3} \,. \tag{27}$$

Here the observed value of $\boldsymbol{C}(R_\infty)$ is based on the study of Ramanathan et al. (1989), and the observed value of LP is based on the globally averaged precipitation rate of 3 mm day^{-1}(e.g.,

Peixóto and Oort, 1990). This nondimensional parameter, β, measures the value of $\boldsymbol{C}(R_\infty)$, relative to the rate of latent heat release. Roughly speaking, the value of β tells how much cirrus cloud is produced per unit of precipitation. Substitution of (26) and (27) into (25) gives

$$LP = \frac{-(SW_{atmclr} - LW_{atmclr})}{1+\beta}. \tag{28}$$

The (positive) numerator of (28) is the net clear-sky atmospheric radiative cooling. Equation (28) shows that as β increases, the globally averaged precipitation rate decreases. In other words, *the more cirrus is produced per unit precipitation rate, the slower the hydrologic cycle must run*. In view of the importance of hydrologic processes for the climate system, the value of β is a very important index of the climate state. It increases as the global precipitation efficiency decreases. To see this, write

$$W = P + C. \tag{29}$$

Here W indicates the rate at which water vapor is condensed to form clouds, P is the precipitation rate, and C is the rate of cloud-water formation. The precipitation efficiency can be defined as

$$\eta \equiv \frac{P}{W}. \tag{30}$$

From (29) we see that

$$\frac{1}{\eta} = 1 + \frac{C}{P} \sim 1 + \beta . \tag{31}$$

Here we have used the fact that $\frac{C}{P}$ is analogous to β. Then we find that

$$\eta \sim \frac{1}{1+\beta} . \tag{32}$$

According to (32), as β increases, the precipitation efficiency decreases.

Suppose that the hydrologic cycle undergoes a positive fluctuation, i.e., that the globally averaged rates of precipitation and evaporation increase for some reason. An increase in the speed of the hydrologic cycle[4] will tend to produce an increase in the amount of cirrus cloud cover, at least in the vicinity of the precipitation event(s). The cirrus can then spread over a large region. From this perspective, we would expect $-\mathcal{C}(R_\infty)$ and LP to increase together, which suggests that β might tend to remain roughly constant.

On the other hand, an increase in $-\mathcal{C}(R_\infty)$ will cause the net atmospheric radiative cooling to decrease. In order to maintain global atmospheric energy balance, the precipitation rate will have to decrease; the initial fluctuation of the hydrologic cycle will, therefore, be damped. From this perspective, we would expect LP to decrease as $-\mathcal{C}(R_\infty)$ increases. This would imply an increase in β.

To the extent that LP decreases as $-\mathcal{C}(R_\infty)$ increases, our hypothesized positive fluctuation of the globally averaged hydrologic cycle will be damped. This is a negative

4. The speed of the hydrologic cycle is measured by the globally averaged rates of evaporation and precipitation, which must balance in equilibrium.

feedback, which can be called a "global radiative-convective feedback" (Fowler and Randall, 1994). This negative feedback will tend to regulate the speed of the hydrologic cycle. It is a cloud feedback, because it involves both cloud formation (principally cirrus formation) and precipitation.

Note that this conclusion would be bolstered, rather than weakened, if clouds absorb a significant amount of solar radiation.

Note, however, that a decrease in LP could lag the increase in $-C(R_\infty)$ by days or weeks. In contrast, upper tropospheric cloudiness responds almost immediately to an increase in convective activity. This disparity in time scales between cloud formation and the effects of clouds on the thermal structure of the atmosphere may make it difficult for the system to settle into a steady state.

7. The thermostat feedback

Ramanathan and Collins (1991) pointed out that deep convection occurs preferentially over the warmest waters of the western tropical Pacific Ocean, and that the convection produces optically thick cloud masses which reflect much of the locally incident solar radiation back to space. Most of this radiation would otherwise be absorbed by the ocean. Ramanathan and Collins also used data from the Earth Radiation Budget Experiment (ERBE; Barkstrom et al. 1989) to demonstrate that when El Niño causes the SSTs of the western tropical Pacific to decrease, and those of the central and eastern tropical Pacific to increase, the strongest deep convection "follows" the warm water eastward, so that the high-albedo clouds follow the warmest water. Ramanathan and Collins suggested that the tendency of strong SW CRF to occur over the warm water amounts to a "thermostat" which tends to limit the warmest SSTs that can occur on the Earth to values in the neighborhood of 305 K. It has been speculated that a similar "thermostat effect" may act globally to regulate the globally averaged surface temperature of the Earth.

A key ingredient of the thermostat hypothesis is the idea that there exists a "threshold" SST above which deep convection is favored. As is well known (e.g., Bjerknes, 1969; Graham and Barnett, 1987), the present climate of the Earth is in fact characterized by a threshold SST for the onset of deep convection; this temperature is in the neighborhood of 300 or 301 K. When the local sea surface temperature exceeds this threshold value, deep convection (i.e., reaching the tropical tropopause) is often observed to be widespread, but at colder temperatures, deep convection is observed to be relatively rare.

We can imagine that the threshold SST might be a "universal constant," in the sense that it would be the same on either a warmer or colder Earth. An alternative possibility is that the threshold temperature is a property of the climatic state, increasing when the climate undergoes a general warming, and decreasing when it undergoes a general cooling. We have investigated the universality of the threshold SST using a suite of AGCMs, which have different convection parameterizations, different stratiform cloudiness algorithms, and so on. The models used are listed in Table 1, which summarizes some particularly relevant aspects of each model's formulation.We have performed three July runs with each AGCM: a control run in which the SST is not perturbed, a "+2 K" run in which the SST is uniformly increased by 2 K relative to the control run, and a "-2 K" run in which the SST is uniformly decreased by 2 K relative to the control. The experimental design thus follows that of C89.

The results are summarized in Fig. 8. Each panel of the figure depicts a probability density function. The horizontal axis is the sea surface temperature, and the vertical axis is the TOA outgoing LW radiation (OLR), with the smaller values at the bottom and the larger values at the top. The center column shows the observations (top) and the AGCM results for the control runs. The left column shows the AGCM results of the -2 K runs, and the right column shows the AGCM results of the +2 K runs. The results of the control runs are generally consistent with the observations, indicating the existence of a threshold SST for the current climate, as discussed above. In the +2 K runs, the SST threshold has increased by 2 K, and in the -2 K runs it has

Model	Cumulus parameterization	Stratiform cloud parameterization	Boundary-layer parameterization
CSU	Prognostic Arakawa-Schubert, with multiple cloud bases	Eauliq; Fowler et al. (1996)	Explicit boundary layer identified as the lowest model layer
DNM	Betts-Miller scheme; Betts (1986)	Slingo scheme; Slingo (1987)	Six levels in the boundary layer
ECMWF	Tiedtke (1989)	Tiedtke (1993)	Louis et al. (1982)
GFDL	Moist convective adjustment	Large-scale saturation	
MGO	Kuo and Arakawa-Schubert, in alternative versions (Meleshko et al., 2000)	Cloud amount parameterized in terms of relative humidity (Shneerov et al., 1997)	Boundary layer represented the four lowest layers (Shneerov et al., 1997)
UIUC	Modified Arakawa-Schubert with prognostic cloud water and diagnostic cloud cover (Oh, 1989; Schlesinger et al., 1997; Wang and Schlesinger, 1999)	Modified Sundqvist, with prognostic cloud water and diagnostic cloud cover (Oh, 1989; Schlesinger et al., 1997; Wang and Schlesinger, 1999)	Boundary layer represented the four lowest layers (Oh, 1989; Schlesinger et al., 1997; Wang and Schlesinger, 1999)

Table 1: Summary of the AGCMs used in the SST threshold study.

decreased by 2 K. Inspection of the results for the simulated precipitation rate (not shown) confirms these results.

We conclude that the threshold SST is a function of the climatic state; it is not universal. Observational evidence in support of this conclusion was reported by Bajuk and Leovy (1998).

8. Cloud feedback, water-vapor feedback, and the tropical general circulation

It is widely but not universally agreed that there exists a positive "water-vapor feedback" which amplifies climate variability. As summarized by Ramanathan (1981), the mechanism of a positive water-vapor feedback is as follows: If an external forcing such as an increased CO_2 concentration tends to produce a warming of the SST, this will tend to cause an increase in surface evaporation, which in turn will lead to an increase in the amount of water vapor in the atmosphere. Because water vapor is a strong greenhouse gas, this increase in the atmospheric

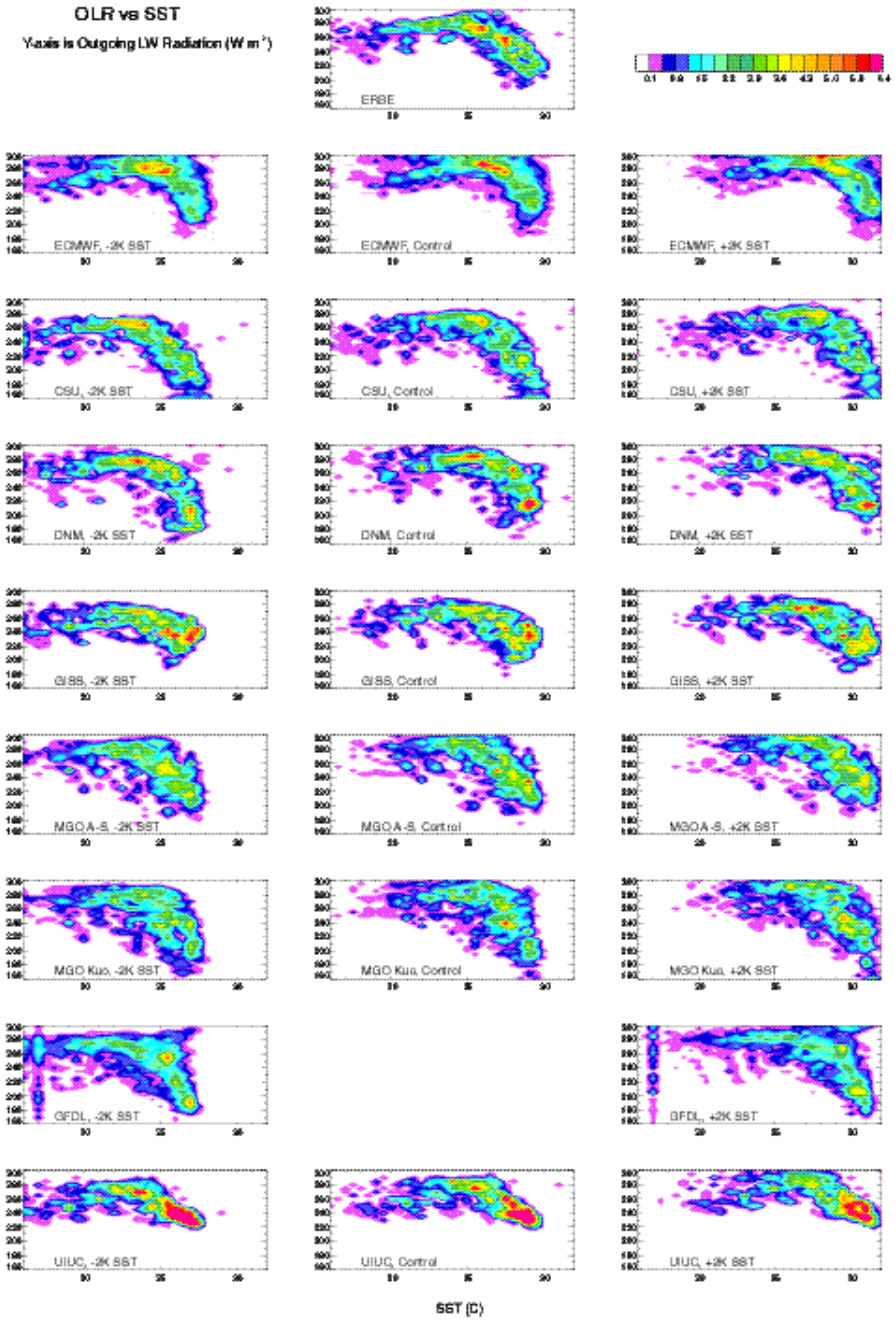

Fig. 8: **Each panel depicts a probability density function. The horizontal axis is the sea surface temperature, and the vertical axis is the TOA OLR, with the smaller values at the bottom and the larger values at the top. The center column shows the observations (top) and the AGCM results for the control runs. The left column shows the AGCM results of the -2 K runs, and the right column shows the AGCM results of the +2 K runs.**

water-vapor content will cause an increase in the downwelling infrared radiation at the Earth's surface, thus favoring a further increase in the SST and, therefore, a positive feedback on the initial warming.

Surface evaporation can continue only if a mechanism exists to carry water vapor upward away from the surface. Boundary-layer turbulence can do this, but only through the depth of the boundary layer, which is typically less than 1 km. In any case, the air near the boundary-layer top is typically near saturation over the tropical oceans. Further lifting of moisture, beyond the boundary-layer top, is necessary if the total moisture content of the atmospheric column is to increase significantly. The most important mechanism for such further lifting is cumulus convection. It follows that convective clouds play an essential role in the "water vapor" feedback (Emanuel and Zivkovic-Rothman, 1999).

Lindzen (1990) argued that if convection penetrates to higher levels in a warmer climate, the air near cloud-top will be colder and will therefore have a lower saturation mixing ratio for water vapor. The air detrained from cumulus towers will, therefore, contain less water vapor. He suggested that as a result the upper troposphere will be drier if the surface temperature warms, and on this basis he questioned the sign of the water-vapor feedback. He pointed out that upper-tropospheric water vapor can strongly affect the Earth's radiation budget, even though the amount of water vapor in the upper troposphere is much smaller than that in the lower troposphere. He argued that a drying of the upper troposphere in a warmer climate would, therefore, significantly reduce the magnitude of a positive water-vapor feedback, and might even give rise to a negative water-vapor feedback. Lindzen's hypothesis of small or negative water-vapor feedback has been met with considerable skepticism (e.g., Held and Soden, 2000), but it has stimulated a lot of useful research by drawing attention to the radiative importance of upper-tropospheric water vapor, and to the importance of deep moist convection for affecting the amount of upper-tropospheric water vapor.

There is an emerging view of the tropical general circulation (Pierrehumbert, 1995; Miller, 1997; Larson et al., 1999; Nilsson and Emanuel, 1999; Sherwood, 1999; Kelly and Randall, 2000) which holds that the magnitude of the mass-transport in the Hadley and Walker circulations is driven by clear-sky radiative cooling in the convectively inactive regions of the tropics, rather than by latent-heat release in the convectively active regions. Following Pierrehumbert (1995), we conceptually divide the tropics into "Warm Pool" and "Cold Pool" regions, as depicted in Fig. 9. The Warm Pool atmosphere is characterized by large-scale rising

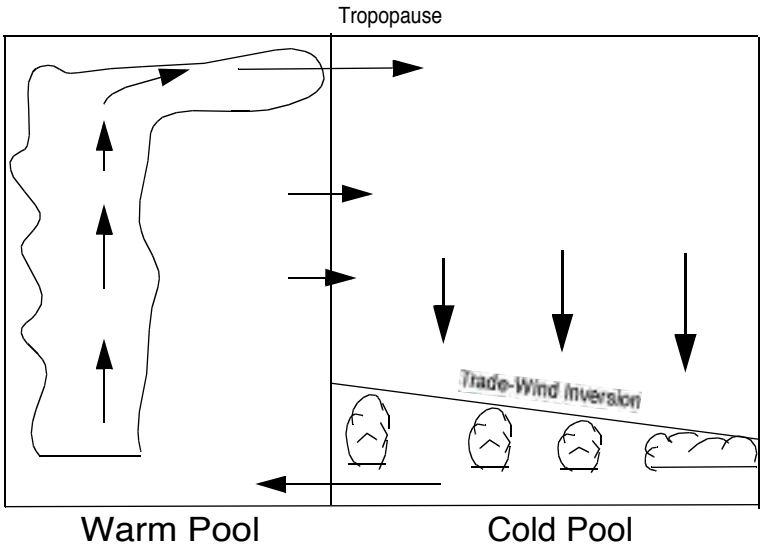

Fig. 9: **A simplified conceptual model of the Walker Circulation. The domain is divided into a Warm Pool region on the west and a Cold Pool region on the east. Deep convection occurs over the Warm Pool. Only shallow, low-level clouds occur over the Cold Pool. See text for details.**

motion, deep moist convection, and high relative humidities throughout the troposphere. Within the Warm Pool atmosphere, strong moist convection ensures that the temperature sounding closely approximates a saturated moist adiabat which passes through the surface temperature and pressure. Large-scale dynamical effects impose this same convectively determined temperature sounding on the middle- and upper-troposphere of the Cold-Pool atmosphere (Charney, 1963).

The deep convection of the Warm Pool moistens the entire column and produces abundant upper-tropospheric cloudiness which is associated with a net radiative warming of the atmospheric column (Stephens and Webster, 1979), primarily due to the blocking of upwelling longwave radiation from the surface and the lower troposphere. The radiative effects of these clouds can even affect the stratosphere and the tropopause height. Kelly et al. (1999) considered a stratosphere in radiative equilibrium above a convectively active tropospheric column. They showed that the cloud-induced reduction of the upward LW radiation across the tropopause leads to a cooling of the stratosphere, which in turn permits deeper penetration of the convective towers and so leads to a higher tropopause.

In the middle and upper troposphere, air flows outward from the Warm Pool to the Cold Pool, carrying the water-vapor-mixing-ratio profile impressed by the deep convection of the Warm Pool. This air then gradually subsides, bringing very dry upper tropospheric air down into the lower and middle troposphere of the Cold Pool region (Salathé and Hartmann, 1997). The rate of subsidence in the Cold-Pool free troposphere (above the tradewind inversion) is determined by a thermodynamic balance between subsidence and radiative cooling:

$$\omega \frac{\partial \theta}{\partial p} \cong \frac{\theta}{c_p T} Q_R , \tag{33}$$

where ω is the vertical pressure velocity, p is pressure, θ is the potential temperature, c_p is the specific heat of air at constant pressure, T is temperature, and Q_R is the radiative heating rate, which is typically negative over the Cold Pool due to dominant emission of infrared radiation by the subsiding air. As discussed above, $\frac{\partial \theta}{\partial p}$ is impressed on the Cold Pool by the convective physics of the Warm Pool, in combination with large-scale dynamical processes discussed by Charney (1963). Therefore, for a given value of Q_R, Eq. (33) essentially determines the vertical velocity,

ω .

Now recall that the radiative cooling rate in the middle and upper troposphere is strongly influenced by the water-vapor content of the air. It follows that the rate of subsidence in the Cold Pool is controlled by the water vapor content of the air flowing from the Warm Pool to the Cold Pool, and this is largely determined by convective cloud processes at work in the Warm Pool region.

The total subsiding mass flux over the Cold Pool is essentially the vertical velocity times the width of the Cold Pool. To the extent that the width of the Cold Pool is fixed, the subsiding mass flux over the Cold Pool is determined by Q_R which, in turn, is determined by the water-vapor content of the subsiding air. Likewise, the total rate of radiative energy loss over the Cold Pool is Q_R times the width of the Cold Pool. To first order, the total radiative energy loss from the Cold Pool must be balanced by latent heat release over the Warm Pool. The relative widths of the Cold Pool and Warm Pool must adjust so that this overall energy balance is maintained. Further discussion is given by Kelly and Randall (2000).

This perspective on the tropical general circulation emphasizes the roles of clouds and water vapor, and the interactions of radiation with the large-scale dynamics. From this point of view, cloud feedbacks play an essential role in the basic dynamics of the tropical circulation, in addition to their roles in climate change.

9. A look ahead

The early global atmospheric circulation models of the 1960s and 1970s prescribed the distribution of cloudiness. During those same years, observations of the global distribution of clouds and their effects on the radiation budget and the hydrologic cycle were also very crude or non-existent.

During the 1980s, the importance of clouds for climate achieved near-universal acceptance. At the same time, our observations of cloudiness improved drastically with the advent of the International Cloud Climatology Project (ISCCP; Rossow and Schiffer, 1999) and the Earth Radiation Budget Experiment (ERBE; Barkstrom et al., 1989), as well as FIRE (e.g., Randall et al., 1995).

During the 1990s, the cloud parameterizations used in climate models were drastically improved through the introduction of explicit cloud water and cloud ice variables which directly link the simulated hydrologic and radiative processes (e.g., Tiedtke 1993; Fowler et al. 1996; Del Genio et al., 1996). Our observational capabilities have also improved during the 1990s, through such efforts as ARM (Stokes and Schwartz, 1994), LITE (McCormick et al. 1993), TRMM (Simpson et al., 1996), and CERES (Wielicki et al. 1996). Nevertheless, the global atmospheric models have advanced so rapidly that, as we enter the new century, the models can simulate aspects of global cloudiness (e.g., the seasonally and synoptically and diurnally varying three-dimensional distribution of ice water content) which are beyond our power to observe; in this sense, the models are "ahead of" the observations.

Later in this decade, however, new satellite systems such as CloudSat (Miller and Stephens, 2000; Stephens et al., 2000), Picasso-CENA (Winker and Wielicki, 1999), and the proposed TRMM follow-on mission (National Aeronautics and Space Administration, 2000) will provide unprecedented data on the vertical structures and meso- and micro-scale structures of cloud systems and their ice and cloud water contents, as well as the global distribution of precipitation. With the advent of these data, the observations may well race ahead of the global models, challenging the modeling community to simulate the newly observed structures and inter-relationships.

This see-saw battle between observations and simulations is bringing about a revolution in our understanding of the role of clouds of all kinds in the climate system, and it will permit both measurement and understanding of the nature and role of cloud feedback on time scales

ranging from hours out to a few decades. We will be able to document, and we will try to understand, both transient fluctuations and persistent trends. Will the marine stratocumulus and SST trends shown in Fig. 3 continue and intensify over the coming decades? Will the hydrologic cycle accelerate while the climate warms, as current climate simulations strongly suggest? Will the upper troposphere moisten or dry? Will the Cold Pool warm in a perpetual El Niño? We are going to find out, and when we do we will see the changes in cloudiness which accompany these climate shifts. Cloud-climate feedbacks will become manifest in our data. We can't wait.

Acknowledgements

Anthony Del Genio provided the GISS GCM results shown in Section 7.

This research has been supported by the National Aeronautics and Space Administration through contract NAS1-98125 and grant NAG1-2081; by the National Science Foundation through grant ATM-9812384; and by the U. S. Department of Energy's ARM Program, through grant number DE-FG03-95ER61968, all to Colorado State University. Support has also been provided by the Russian Fund for Basic Research through Grant 99-06-66274.

Thanks to Graeme Stephens for helpful discussions. Mark Branson and Don Dazlich assisted with some of the plots. Byron Boville and Jim Hack assisted in accessing the CCSM results.

References

Arakawa, A., and W. H. Schubert, 1974: The interaction of a cumulus cloud ensemble with the large-scale environment, Part I. *J. Atmos. Sci.*, **31**, 674-701.

Arakawa, A., 1975: Modeling clouds and cloud processes for use in climate models. In *The Physical Basis of Climate and Climate Modelling*. GARP Publications Series No. 16, 181-197, ICSU/WMO, Geneva.

Bajuk, L. J., and C. B. Leovy, 1998: Seasonal and interannual variations in stratiform and convective clouds over the tropical Pacific and Indian Oceans from ship observations. *J. Climate*, **11**, 2922-2941.

Barkstrom, B., E. F. Harrison, G. L. Smith, R. N. Green, J. Kibler, R. Cess, and the ERBE Science Team, 1989: Earth Radiation Budget Experiment (ERBE) archival and April 1985 results. *Bull. Amer. Meteor. Soc.*, **74**, 591-598.

Betts, A. K., 1986: A new convective adjustment scheme. Part I. Observational and theoretical basis. *Quart. J. Roy. Meteor. Soc.*, **112**, 677-691.

Bjerknes, J., 1969: Atmospheric teleconnections from the equatorial Pacific. *Mon. Wea. Rev.*, **97**, 163-172.

Bode, H. W., 1975: *Network analysis and feedback amplifier design*. Krieger, 577 pp.

Boville, B. A., and P. R. Gent, 1998: The NCAR Climate System Model, version one. *J. Climate*, **11**, 1115-1130.

Cess, R. D., 1976: Climate change: an appraisal of atmospheric feedback mechanisms employing zonal climatology. *J. Atmos. Sci.*, **33**, 1831-1843.

Cess, R. D., G. L. Potter, J. P. Blanchet, G. J. Boer, S. J. Ghan, J. T. Kiehl, H. Le Treut, Z.-X. Li, X.-Z. Liang, J. F. B. Mitchell, J.-J. Morcrette, D. A. Randall, M. Riches, E. Roeckner, U. Schlese, A. Slingo, K. E. Taylor, W. M. Washington, R. T. Wetherald, and I. Yagai, 1989: Interpretation of cloud-climate feedback as produced by 14 atmospheric general circulation models. *Science*, **245**, 513-516.

Cess, R. D., G. L. Potter, J. P. Blanchet, G. J. Boer, A. D. Del Genio, M. Deque, V. Dymnikov, V. Galin, W. L. Gates, S. J. Ghan, J. T. Kiehl, A. Lacis, H. Le Treut, Z.-X. Li, X.-Z. Liang, B.

J. McAvaney, V. P. Meleshko, J. F. B. Mitchell, J.-J. Morcrette, D. A. Randall, L. Rikus, E. Roeckner, J. F. Royer, U. Schlese, D. A. Sheinin, A. Slingo, A. P. Sokolov, K. E. Taylor, W. M. Washington, R. T. Wetherald, I. Yagai, and M.-H. Zhang, 1990: Intercomparison and interpretation of climate feedback processes in 19 atmospheric general circulation models. *J. Geophys. Res.*, **95**, 16601-16615.

Cess, R. D., M. H. Zhang, G. L. Potter, V. Alekseev, H. W. Barker, E. Cohen-Solal, R. A. Colman, D. A. Dazlich, A. D. Del Genio, M. R. Dix, V. Dymnikov, M. Esch, L. D. Fowler, J. R. Fraser, V. Galin, W. L. Gates, J. J. Hack, W. J. Ingram, J. T. Kiehl, H. Le Treut, K. K.-W. Lo, B. J. McAvaney, V. P. Meleshko, J.-J. Morcrette, D. A. Randall, E. Roeckner, J.-F. Royer, M. E. Schlesinger, P. V. Sporyshev, B. Timbal, E. M. Volodin, K. E. Taylor, W. Wang, and R. T. Wetherald, 1996: Cloud Feedback in Atmospheric General Circulation Models: An Update. *J. Geophys. Res.*, **101**, 12791-12794.

Cess, R. D., M. H. Zhang, G. L. Potter, V. Alekseev, H. W. Barker, S. Bony, R. A. Colman, D. A. Dazlich, A. D. Del Genio, M. Déqué, M. R. Dix, V. Dymnikov, M. Esch, L. D. Fowler, J. R. Fraser, V. Galin, W. L. Gates, J. J. Hack, W. J. Ingram, J. T. Kiehl, Y. Kim, H. Le Treut, X. Z. Liang, B. J. McAvaney, V. P. Meleshko, J.-J. Morcrette, D. A. Randall, E. Roeckner, M. E. Schlesinger, P. V. Sporyshev, K. E. Taylor, B. Timbal, E. M. Volodin, W. Wang, W. C. Wang, and R. T. Wetherald, 1997: Comparison of atmospheric general circulation models to satellite observations of the seasonal change in cloud-radiative forcing. *J. Geophys. Res.*, **102**, 16593-16604.

Charney, J. G., 1963: A note on large-scale motion in the tropics. *J. Atmos. Sci.*, **20**, 607-609.

Charney, J. G., 1979: Carbon dioxide and climate: A scientific assessment. National Academy Press, Washington, D. C., 33 pp.

Curry, J. C., and P. J. Webster, 1999: *Thermodynamics of atmospheres and oceans*. International Geophys. Ser., 65, Academic Press, 471 pp.

Dai, A., T. M. L. Wigley, B. Boville, J. T. Kiehl, and L. Buja, 2000: Climates of the 20th and 21st centuries simulated by the NCAR Climate System Model. Submitted to *J. Climate*.

Del Genio, A. D., M.-S. Yao, W. Kovari, and K. K.-W. Lo, 1996: A prognostic cloud water parameterization for global climate models. *J. Climate*, **9**, 270-304.

Emanuel, K. A., and M. Zivkovic-Rothman, Marina, 1999: Development and evaluation of a convection scheme for use in climate models. *J. Atmos. Sci.*, **56**, 1766-1782.

Fowler, L. D., and D. A. Randall, 1994: A global radiative-convective feedback. *Geophys. Res. Lett.*, **21**, 2035 - 2038.

Fowler, L. D., D. A. Randall, and S. A. Rutledge, 1996: Liquid and Ice Cloud Microphysics in the CSU General Circulation Model. Part 1: Model Description and Simulated Microphysical Processes. *J. Climate*, **9**, 489-529.

Graham, N. E., and T. P. Barnett, 1987: Observations of sea-surface temperature and convection over tropical oceans. *Science*, **238**, 657-659.

Hall, A., and S. Manabe, 1999: The Role of Water Vapor Feedback in Unperturbed Climate Variability and Global Warming. *J. Climate*, **12**, 2327–2346.

Held, I., and B. J. Soden, 2000: Water vapor feedback and global warming. *Annual Reviews of Energy and the Environment*, **25** (to appear).

Hendon, H. H., and K. Woodberry, 1993: The diurnal cycle of tropical convection. *J. Geophys. Res.*, **98**, 16623-16637.

Houghton, J. T., G. J. Jenkins, and J. J. Ephraums, Eds., 1990: *Climate Change. The IPCC Scientific Assessment*. World Meteorological Organization / United Nations Environment Programme. Cambridge University Press.

Kelly, M. A., D. A. Randall, and G. L. Stephens, 1999: A simple radiative-convective model with a hydrologic cycle and interactive clouds. *Quart. J. Roy. Met. Soc.,* **125**, 837-869.

Kelly, M. A., and D. A. Randall, 2000: The effects of the vertical distribution of water vapor on the strength of the Walker Circulation. Submitted to *J. Climate*.

Klein, S. A., and C. Jakob, 1999: Validation and sensitivities of frontal clouds simulated by the ECMWF model. *Mon. Wea. Rev.*, **127**, 2514–2531.

Larson, K., D. L. Hartmann, and S. A. Klein, 1999: Climate sensitivity in a two box model of the tropics. *J. Climate*, **12**,2359-2374.

Lilly, D. K., 1968: Models of cloud-topped mixed layers under a strong inversion. *Quart. J. Roy. Meteor. Soc.*, **94**, 292-309.

Lin, X., D. A. Randall, and L. D. Fowler, 2000: Diurnal Variability of the Hydrologic Cycle and Radiative Fluxes: Comparisons Between Observations and a GCM. *J. Climate* (to appear).

Lindzen, R. S., 1990: Some coolness concerning global warming. *Bull. Amer. Meteor. Soc.*, **71**, 288-299.

Louis, J. F., M. Tiedtke, and J. F. Geleyn, 1982: A short history of the operational planetary boundary layer parameterization at ECMWF. *Workshop on Planetary Boundary Layer Parameterization*, European Centre for Medium Range Weather Forecasts, 59-79, 260 pp.

McCormick, M. P., D. M. Winker, E. V. Browell, J. A. Coakley, C. S. Gardner, R. M. Hoff, G. S. Kent, S. H. Melfi, R. T. Menzies, C. M. R. Platt, D. A.Randall, and J. A. Reagan, 1993:

Science Investigations Planned for the Lidar In-Space Technology Experiment (LITE). *Bull. Amer. Meteor.Soc.*, **74**, 205 - 214.

Manabe, S., and K. Bryan, 1969: Climate calculation with a combined ocean-atmosphere model. *J. Atmos. Sci.*, **26**, 786-789.

Meleshko, V. P., V. M. Katsov, P. V. Sporysev, S. V. Vavulin, and V. A. Govorkova, 2000: Feedbacks in the climate system: Cloud, water vapour, and radiation interaction. *Meteorologia and Gidrolagia*, **2**, 22-45.

Miller, R. L., 1997: Tropical thermostats and low cloud cover. *J. Climate*, **10**, 409-440.

Miller, S. D, G. L. Stephens, G. L., and A. C. M. Beljaars, 1999: A validation survey of the ECMWF prognostic cloud scheme using LITE. *Geophys. Res. Lett.*, **26**, 1417-1420.

Miller, S. D., and G. L. Stephens, 2000; CloudSat Instrument Requirements as determined from ECMWF Forecasts of Global Cloudiness. Submitted to *J. Geophys. Res.*

Mitchell, J. F. B., C. A. Senior, and W. J. Ingram, W. J., 1989: CO_2 and climate: A missing feedback. *Nature*, **341**, 132-134.

Mitchell, J. F. B., and W. J. Ingram, 1992: Carbon dioxide and climate: mechanisms of changes in cloud. *J. Climate*, **5**, 5-21.

National Aeronautics and Space Administration, 2000: *Understanding Earth System Change: NASA's Earth Science Enterprise Research Strategy 2000-2010*. Available from the Earth Science Enterprise Office of the National Aeronautics and Space Administration (additional bibliographic information to be provided).

Nilsson, J., and K. A. Emanuel, K. A., 1999: Equilibrium atmospheres of a two-column radiative-

convective model. *Quart. J. Roy. Meteor. Soc.*, **125**, 2239-2264.

Norris, J. R., and C. B. Leovy, 1994: Interannual variability in stratiform cloudiness and sea surface temperature. *J. Climate*, **7**, 1915-1925.

Oh, J.-H., 1989: Physically-Based General Circulation Model Parameterization of Clouds and their Radiative Interaction. Ph. D. dissertation Thesis, Oregon State University, Corvallis, 315 pp.

Peixóto, J. P., and A. H. Oort, 1992: *Physics of Climate*. Amer. Inst. Physics, New York, 520 pp.

Pierrehumbert, R. T., 1995: Thermostats, radiator fins, and the runaway greenhouse. *J. Atmos. Sci.*, **52**, 1784-1806.

Ramanathan, V., 1981: The role of ocean-atmosphere interactions in the CO_2 climate problem. *J. Atmos. Sci.*, **38**, 918-930.

Ramanathan, V., R. D. Cess, E. F. Harrison, P. Minnis, B. R. Barkstrom, E. Ahmad, and D. Hartmann, 1989: Cloud-radiative forcing and climate: Results from the Earth Radiation Budget Experiment. *Science*, **243**, 57-63.

Ramanathan, V. and W. Collins, 1991: Thermodynamic regulation of ocean warming by cirrus clouds deduced from observations of the 1987 El Niño. *Nature*, **351**, 27-32.

Randall, D. A., 1989: Cloud Parameterization for Climate Models: Status and Prospects. *Atmospheric Research*, **23**, 345-362.

Randall, D. A., B. A. Albrecht, S. K. Cox, P. Minnis, W. Rossow, and D. Starr, 1995: On FIRE at Ten. *Adv. Geophys.*, **38**, 37-177.

Rodwell, M. J., and B. J. Hoskins, 2000: Subtropical anticyclones and summer monsoons.

Submitted to *J. Climate*.

Rossow, W. B, and R. A. Schiffer, 1999: Advances in understanding clouds from ISCCP. *Bull. Amer. Meteor. Soc.*, **80**, 2261-2287.

Salathé Jr., E. P. and D. L. Hartmann, 1997: A trajectory analysis of tropical upper-tropospheric moisture and convection. *J. Climate*, **10**, 2533-2547.

Schlesinger, M. E., 1985: Feedback analysis of results from energy balance and radiative-convective models. In "*The potential climatic effects of increasing carbon dioxide*". M. C. MacCracken and F. M. Luther, Eds., U.S. Department of Energy, DOE/ER-0237, pp. 280-319. (Available from NTIS, Springfield, Virginia.)

Schlesinger, M. E., 1988: Quantitative analysis of feedbacks in climate model simulations of CO_2-induced warming. In "*Physically-based modeling and simulation of climate and climatic change*". M. E. Schlesinger, Ed., NATO Advanced Study Institute Series, Reidel, Dordrecht, pp. 653-736.

Schlesinger, M. E., 1989: Quantitative Analysis of Feedbacks in Climate Model Simulations in Understanding Climate Change. *Geophysical Monograph 52, IUGG Volume 7*, 177-187

Schlesinger, M. E., N. G. Andronova, B. Entwistle, A. Ghanem, N. Ramankutty, W. Wang and F. Yang, 1997: Modeling and simulation of climate and climate change. In *Past and Present Variability of the Solar-Terrestrial System: Measurement, Data Analysis and Theoretical Models*. Proceedings of the International School of Physics "Enrico Fermi" CXXXIII, Cini Castagnoli, G. and A. Provenzale (Editors). IOS Press, Amsterdam, pp. 389-429.

Schneider, S. H., 1972: Cloudiness as a global climatic feedback mechanism: The effects on radiation balance and surface temperature of variations in cloudiness. *J. Atmos. Sci.*, **29**,

1413-1422.

Senior, C. A., and J. F. B.Mitchell, 1993: Carbon dioxide and climate: the impact of cloud parameterization. *J. Climate*, **6**, 393-418.

Senior, C. A., 1999: Comparison of mechanisms of cloud-climate feedbacks in GCMs. *J. Climate*, **12**, 1480-1489.

Sherwood, S. C., 1999: Feedbacks in a simple prognostic tropical climate model. *J. Atmos. Sci.*, **56**, 2178-2200.

Shneerov, B. E., V. P. Meleshko, A. P. Sokolov, D. A. Sheinin, V. A. Lubanskai, P. V. Sporyshev, V. A. Matjugin, V. M. Katsov, V. A. Govorkova, and T. V. Pavlova, 1997: MGO global atmospheric general circulation model coupled to mixed layer ocean. *Proceedings of the Voeikov Main Geophysical Observatory*, **544**, 3-122.

Simpson, J., C. Kummerow, W.-K. Tao, and R. F. Adler, 1996: On the Tropical Rainfall Measuring Mission (TRMM). *Meteor. Atmos. Phys.*, **60**, 19-36.

Slingo, J.,1987: The development and verification of a cloud prediction scheme for the ECMWF model. *Quart. J. Roy. Meteor. Soc.*, **133**, 899-927.

Stephens, G. L., and P. J. Webster, 1979: Sensitivity of radiative forcing to variable cloud and moisture. *J. Atmos. Sci.*, **36**, 1542-1556.

Stephens, G. L., and co-authors, 2000: The CloudSat mission: A new dimension to space-based observations of clouds and precipitation. In preparation for *Bull. Amer. Meteor. Soc.*

Stokes, G. M., and S. E. Schwartz, 1994: The Atmospheric Radiation Measurement (ARM) Program: Programmatic background and design of the Cloud and Radiation Test Bed. *Bull.*

Amer. Meteor. Soc., **75**, 1201-1221.

Tiedtke, M., 1989: A comprehensive mass flux scheme for cumulus parameterization in large-scale models. *Mon. Wea. Rev.*, **117**, 1779-1800.

Tiedtke, M., 1993: Representation of clouds in large-scale models. *Mon. Wea. Rev.*, **121,** 3040-3061.

Tiedtke, M., 1993: Representation of clouds in large-scale models. *Mon. Wea. Rev.*, **121,** 3040-3061.

Wang, W. and M. E. Schlesinger, 1999: The dependence on convection parameterization of the tropical intraseasonal oscillation simulated by the UIUC 11-layer atmospheric GCM. *J. Climate*, **12**, 1423-1457.

Wielicki, B. A., R. D. Cess, M. D. King, D. A. Randall, and E. F. Harrison, 1995: Mission to Planet Earth: Role of Clouds and Radiation in Climate. *Bull. Amer. Meteor. Soc.*, **76**, 2125-2153.

Wielicki, B. A., B. R. Barkstrom, E. F. Harrison, R. B. Lee III, G. L. Smith, and J. E. Cooper, 1996: Clouds and the Earth's Radiant Energy System (CERES): An Earth Observing System experiment. *Bull. Amer. Meteor. Soc.*, **77**, 853-868.

Winker and B. A. Wielicki, 1999: The PICASSO-CENA Mission. In *Sensors, Systems, and Next-Generation Satellites III*. (Europto Series) *Proceedings of SPIE,* **3870**, 26-36.

Yao, M.-S., and A. D. Del Genio, 1999: Effects of cloud parameterization on the simulation of climate changes in the GISS GCM. *J. Climate*, **12**, 761-779.